Hindawi Publishing Corporation
International Journal of Geophysics
Volume 2015, Article ID 369143, 11 pages
http://dx.doi.org/10.1155/2015/369143

Research Article

3D Geometric Modeling of the Abu Madi Reservoirs and Its Implication on the Gas Development in Baltim Area (Offshore Nile Delta, Egypt)

Mohamed I. Abdel-Fattah[1] and Ahmed Y. Tawfik[2]

[1]*Geology Department, Faculty of Science, Suez Canal University, Ismailia, Egypt*
[2]*Geology Department, Faculty of Science, Suez University, Suez, Egypt*

Correspondence should be addressed to Mohamed I. Abdel-Fattah; mabdelfattah99@gmail.com

Received 7 July 2014; Revised 27 December 2014; Accepted 29 December 2014

Academic Editor: Marek Grad

3D geometric modeling has received renewed attention recently, in the context of visual scene understanding. The reservoir geometry of the Baltim fields is described by significant elements, such as thickness, depth maps, and fault planes, resulting from an interpretation based on seismic and well data. Uncertainties affect these elements throughout the entire interpretation process. They have some bearing on the geometric shape and subsequently on the gross reservoir volume (GRV) of the fields. This uncertainty on GRV also impacts volumes of hydrocarbons in place, reserves, and production profiles. Thus, the assessment of geometrical uncertainties is an essential first step in a field study for evaluation, development, and optimization purposes. Seismic data are best integrated with well and reservoir information. A 3D geometric model of the Late Messinian Abu Madi reservoirs in the time and depth domain is used to investigate the influence of the reservoir geometry on the gas entrapment. Important conceptual conclusions about the reservoir system behavior are obtained using this model. The results show that the reservoir shape influences the seismic response of the incised Abu Madi Paleovalley, making it necessary to account for 3D effects in order to obtain accurate results.

1. Introduction

The Nile Delta Basin started to show its hydrocarbon potential in the early 1960s. Since then, generations of geologists and geophysicists have applied different concepts and methodologies to explore this area, keeping pace with the latest available technologies. Regional gravity surveys were followed by extended 2D seismic surveys up to almost a routine 3D acquisition in the 1990s [1]. Following this technological and conceptual evolution, the rate of technical success approached almost 100% in the last exploratory phase of the Abu Madi Formation when 3D seismic data and seismic attributes were extensively used to predict the sand distribution within the Abu Madi Paleovalley [1].

Baltim area lies to the north of the Nile Delta between latitudes $31^\circ 37' 25''$ and $31^\circ 56' 19''$N and longitudes $31^\circ 1' 12''$ and $31^\circ 26' 7''$E, about 25 km off the Egyptian Coast. It covers an area of about 500 km^2, with a length of 25 km and a width of 18.75 km (Figure 1). Baltim area is considered as the northwest extension of Abu Madi, El-Qar'a main channel or paleovalley [2]. Inside this erosional feature, the main reservoir bodies of Abu Madi Formation are represented by sandstones, mainly fluvial, developed in the active channel belts as a response to the relative fall/rise of the sea level [3–5]. Due to the discovery of hydrocarbons (gas and oil) in the onshore and offshore areas, a great attention was given to the other parts of the offshore area and high technology of seismic data interpretation is used which led to discovering new and big fields at different depths ranging between 600 and 4000 m and in different formations ages. The area of study is a part of Nile Delta offshore area (Figure 1), which is characterized by the presence of large number of gas fields that have a big amount of reserves from the hydrocarbon point of view [6, 7].

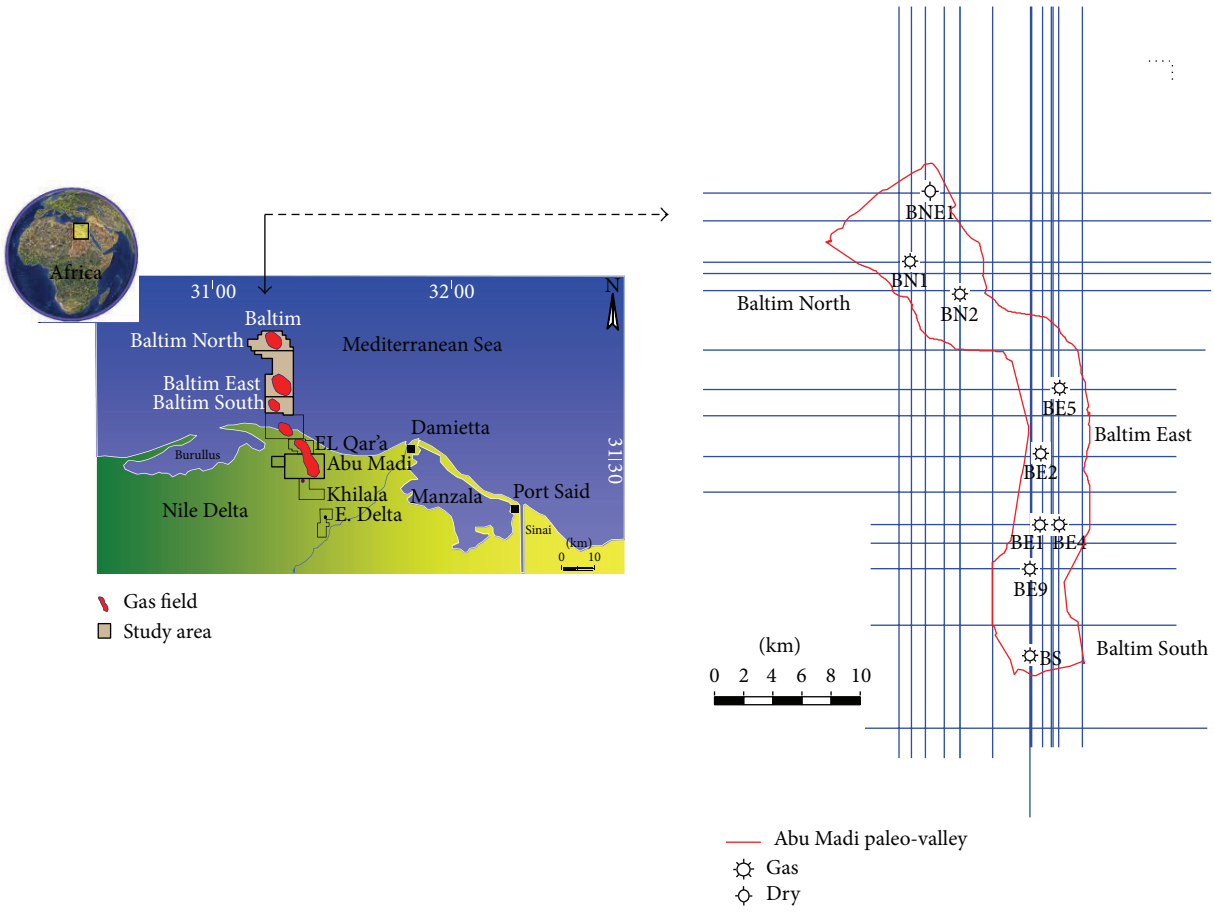

Figure 1: Location map of seismic profiles and wells in the Baltim area (offshore Nile Delta, Egypt).

Baltim East was discovered in 1993 and the production started in April 2000. In the past couple of years some key workovers and a new slanted well (BE10) investigating the northern area of the field, in addition to the good field performance, highlighted the possibility of additional potential in the area and the inadequacy of the available 3D model to correctly simulate the producing behavior. Baltim North was discovered in 1995. The production started only in November 2005 with the tie-in of well BN1. Recently acquired data confirm a complex dynamic relation between the Baltim East and North fields. A new 3D seismic reprocessing has been performed in 2005 merging all the 3D data acquired on the area and producing four angle stack volumes [10].

In order to optimize the development plan in terms of number and placement of wells a detailed reservoir model capturing the complex internal geometry of the reservoir is required. Therefore, the aim of this work is to define the general geological setting of Abu Madi Formation, where gas and condensate accumulation have been trapped, and to construct 3D geometric model of Abu Madi sandstone reservoirs to help in determining the next locations for the future development of Baltim fields.

2. Geological Setting

The Upper Miocene (Messinian) Abu Madi Formation consists mainly of sandstone intercalated with siltstone and shale interbeds. The Abu Madi Formation is a fluviomarine environment [3, 4]. The base of Abu Madi Formation is defined by an unconformity marked by iron oxide stained clays and supported by dipmeter data. Based on the properties of sandstones to silt/mudstone facies, the Abu Madi Formation sands could be divided into three major sand levels, separated by thick silty mud beds. In addition a subordinate sand level could be identified in between levels III and II, being denoted as level III A. These sand levels, mentioned from the older to the younger, are as follows: levels III, III A, II, and I (Figure 2). The core analysis results, ditch cutting description, and well log data, supported the subdivision of level III into three units, which are mentioned from bottom to top as follows: lower, main, and upper level III units [3, 4].

In Baltim area levels III upper unit, III A, II, and I are shale-out. Baltim fields in the offshore Nile Delta are gas-condensate accumulations located in the northern portion of the Abu Madi Paleovalley area [11]. The fields comprise two separate gas pools referred to as the "level III main"

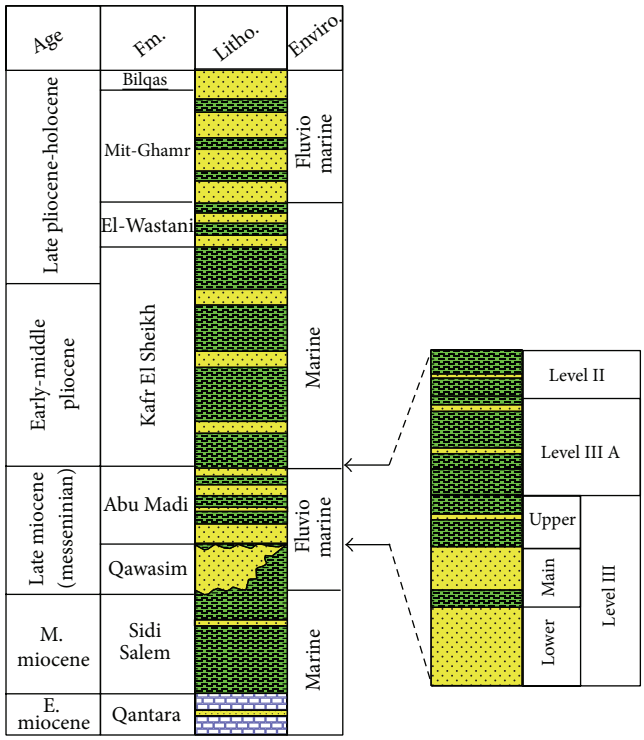

FIGURE 2: Lithostratigraphic column of the Nile Delta in Baltim area, Egypt (modified after [4]).

and "level III lower" within the Late Messinian Abu Madi Formation (Figure 2). Strata of the Abu Madi Formation are interpreted to comprise two sequences [8], which are the most complex stratigraphically; their deposits comprise a complex incised valley fill (Figure 3). The lower sequence (SQ1) consists of a thick incised valley-fill of a lowstand systems tract (LST1) overlain by a transgressive systems tract (TST1) and highstand systems tract (HST1). The upper sequence (SQ2) contains channel-fill and is interpreted as a LST2 which has thin sandstone channel deposits. Above this, channel-fill sandstone and related strata with tidal influence delineate the base of TST2, which is overlain by a HST2.

The general structural setting of the Delta area has been determined using both geophysical methods and well data. The main feature is the Nile Delta Hinge Zone [9], a flexure which affects pre-Miocene formations and extends E-W across the middle of the onshore Delta area, producing step faults (Figure 4). North of the Hinge Zone, large normal faults are the dominant structures. These gravity-induced, "down-to-basin" displacements occur along listric fault planes and have thick Neogene formations which mainly developed in open marine, deep-water facies. The offshore Delta is characterized by a thick, subsidence-controlled sequence of tertiary sediments. South of the Hinge Zone, asymmetric folds of the Syrian Arc Fold System extend along an arcuate trend from northern Sinai and the northern Gulf of Suez, through the southern part of the Delta and into the Western Desert [12]. The basement in this southern area is relatively shallow and block faulting is more common [2].

3. Materials and Methods

3D geometric model of the Abu Madi reservoirs "level III main" and "level III lower" have been done by using Petrel program (Schlumberger's Reservoir Modeling Software). The available data for the current study (Figure 1) are nine composite logs and thirty (2D) seismic profiles that were provided by the Belayim Petroleum Company (BETROBEL), Egypt. To achieve the goal of this study, the following processes and presentations were applied to the available data: well seismic tie, picking horizons and structural features, velocity and depth conversion, and constructing time and depth contour maps, isochore maps, geological model, and 3D geometric model.

3.1. Seismic Well Tie. One of the first steps in interpreting a seismic dataset is to establish the relationship between seismic reflections and stratigraphy [13]. Some wells have sonic (i.e., formation velocity) and formation density logs, at least over the intervals of commercial interest; from these it is possible to construct a synthetic seismogram showing the expected seismic response for comparison with the real seismic data. In addition, some wells have vertical seismic profiling (VSP) data, obtained by shooting a surface seismic source into a downhole geophone, which has the potential to give more precise tie between well and seismic data. Tying well data (in depth) to seismic data (in time) helps to find events (seismic reflections) that correspond to geological formations. There are basically two methods used to tie the geological control into the seismic data: (1) using check shot data, time-depth pairs or (2) using synthetic seismogram. The first method is the simplest but least accurate [14].

Synthetic seismograms are artificial reflection records made from velocity logs by conversion of the velocity log in depth to a reflectivity function in time and by convolution of this function with a presumed appropriate wavelet or source pulse [15]. Generation of the synthetic seismograms was performed using Petrel software. In creating a synthetic seismogram, Petrel software permits the interpreter to tie time data (seismic data) to depth data (well data) by integrating over the velocity profile. Impedance log and reflection coefficients are generated from the velocity and density profiles. The reflection coefficients are convolved with a seismic wavelet to produce a synthetic seismic trace. The synthetic seismogram is then compared with the actual seismic traces at the drill site. The trace at the drill site was compared with adjacent traces to assure that it was representative of that part of the seismic section. Figure 5 shows a typical synthetic seismogram for BE1 well and illustrates the relationship between the impedance logs, reflection coefficients, and synthetic traces for BE1 well. The continuity of the sequence boundary reflections can be observed in this figure. Correlation of the synthetic traces with seismic sections is often helpful in tying a well to a seismic section. Generally, the ties between these synthetic seismograms and the seismic data are satisfactory. The main objective of synthetic seismogram is also to make time-depth relationship. Any changes to the time-depth relationship can be made and seismic horizons can be correlated with the stratigraphic boundaries identified

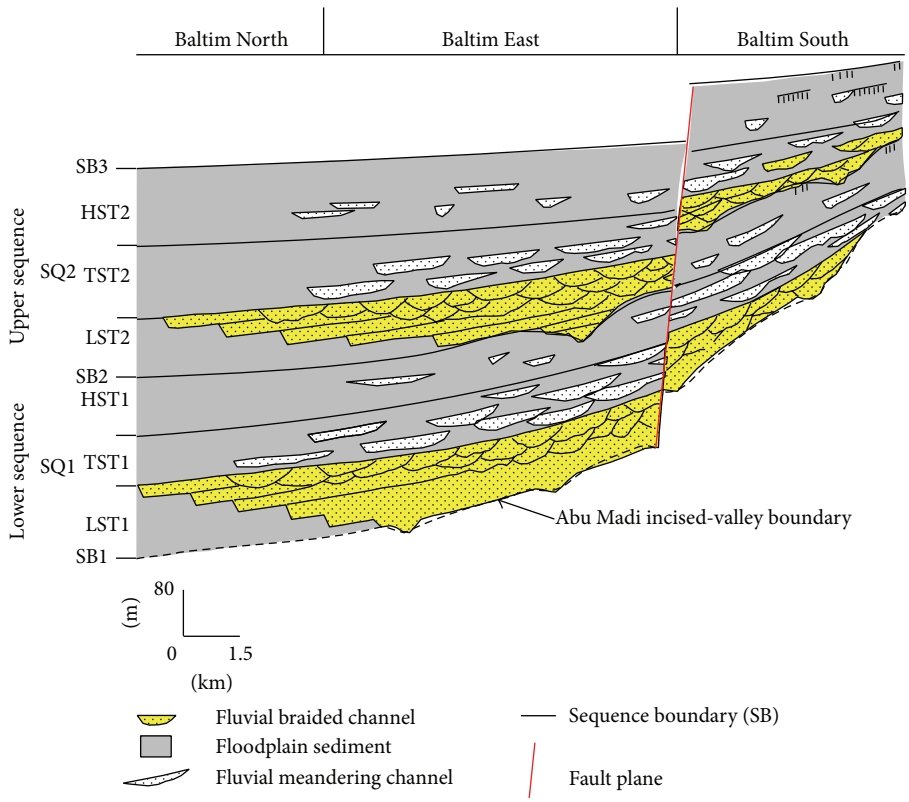

FIGURE 3: Schematic cross section illustrating the sequence stratigraphic framework of the Abu Madi Formation in Baltim fields, offshore Nile Delta, Egypt [8].

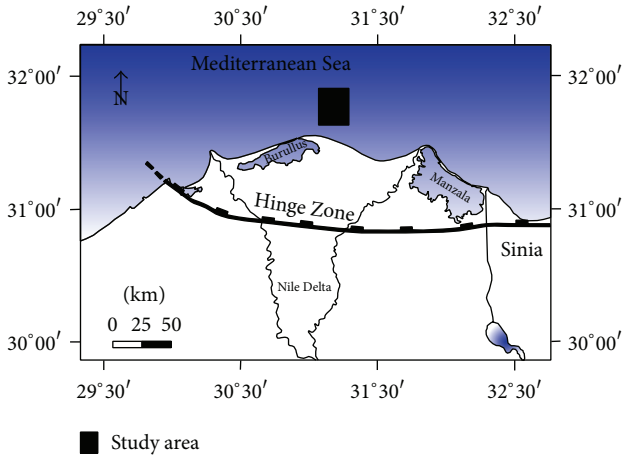

FIGURE 4: Hinge zone structural feature [9].

in wells. When the time-depth relationship has been fine-tuned, all depth indexed well tops will be automatically assigned the updated time value.

3.2. Picking Horizons and Structural Features. Structural interpretation is the most fundamental interpretation activity and includes making maps of horizons and 3D structural model. By correlating specific horizons on a seismic line, it can subsequently generate time data which, after conversion to depth, help generate structural maps (maps which show the geologic structure of a feature) and isochron or isopach maps (maps which show time or thickness of particular intervals, resp.) [16]. These maps are useful in allowing the mapping of particular outlines and in determining the volumes of particular reservoir hydrocarbon accumulations. Based on the well-to-seismic tie the horizons to interpret were chosen in the seismic data. The main attention was focused on the reservoirs intervals, where four horizons were selected to interpret. The selected four horizons for interpretation are bottom Abu Madi, top level III lower, top level III main, and top Abu Madi (Figures 6, 7, 8, and 9). Top and bottom Abu Madi horizons have been chosen to act as structural framework to constrain the level III lower and main reservoirs geometry.

The interpreted horizons in the seismic sections from base to top are as follows (Figures 7 to 9).

(i) Bottom Abu Madi: the interpretation follows a zero crossing value along a strongly angular unconformity at the base of the Abu Madi Fm. While the acoustic contrast strongly changes along this stratigraphic surface, the erosional geometry at its base and onlapping horizons above allows following it (although at times with uncertainty) at a regional scale.

(ii) Top level III lower and top level III main: the interpreted horizon is a seismic peak, locally continuous, whose amplitude is related to decrease in seismic

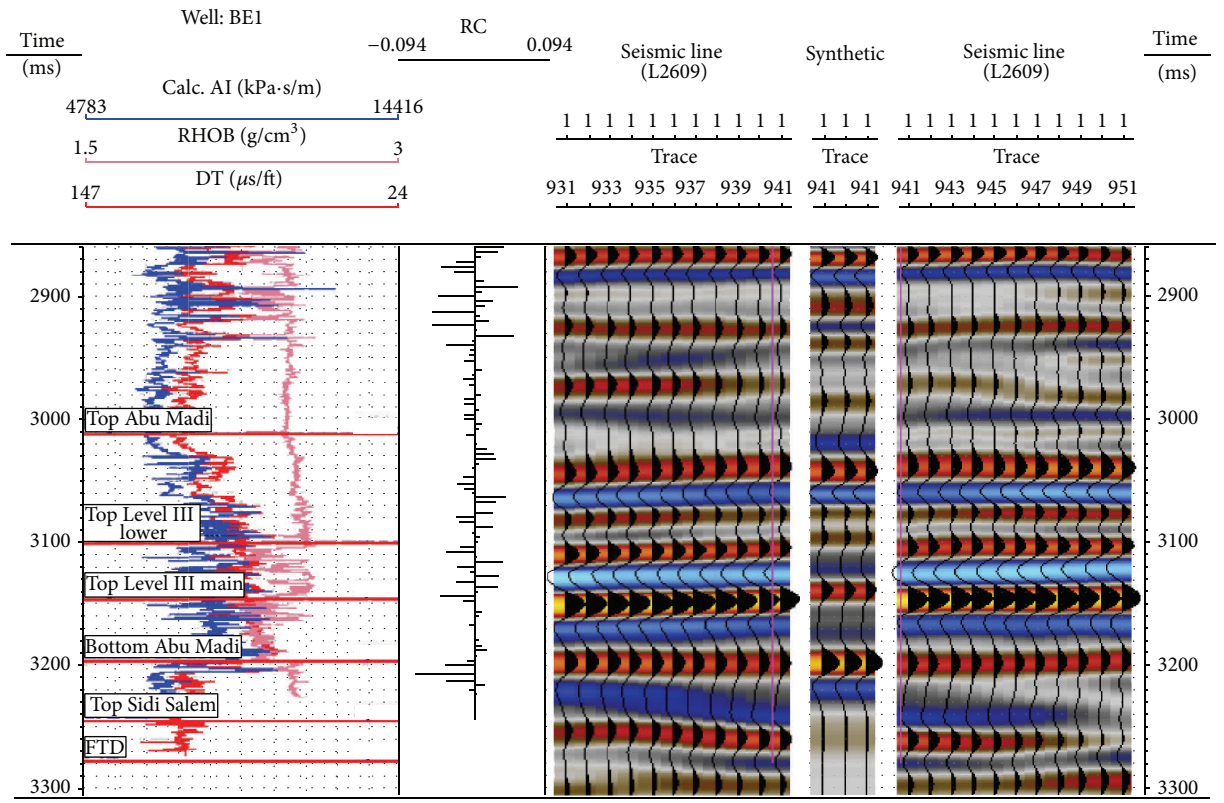

Figure 5: Well BE1, Depth-OWT relationship with linear depth scales. The impedance log, reflection coefficient, and synthetic seismogram generated using the sonic and density logs are included. Part of seismic line 2609 is plotted together with the synthetic seismogram at well BE1.

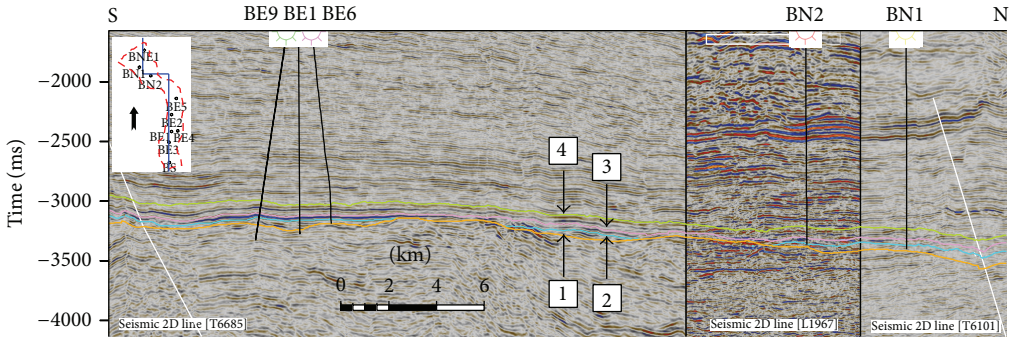

Figure 6: Interpreted arbitrary seismic line consists of T6685, L1967, and T6101, from south to north, showing the main four-horizon area ((1) bottom Abu Madi, (2) top level III lower, (3) top level II main, and (4) top Abu Madi) and the main two faults in the Baltim area.

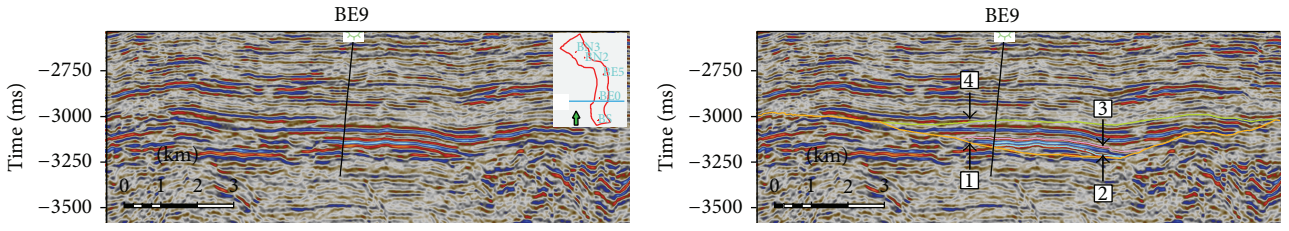

Figure 7: Uninterpreted (a) and interpreted (b) seismic line number (L 2660) passing through Baltim East field from west to east direction, where (1) bottom Abu Madi, (2) top level III lower, (3) top level II main, and (4) top Abu Madi are picked.

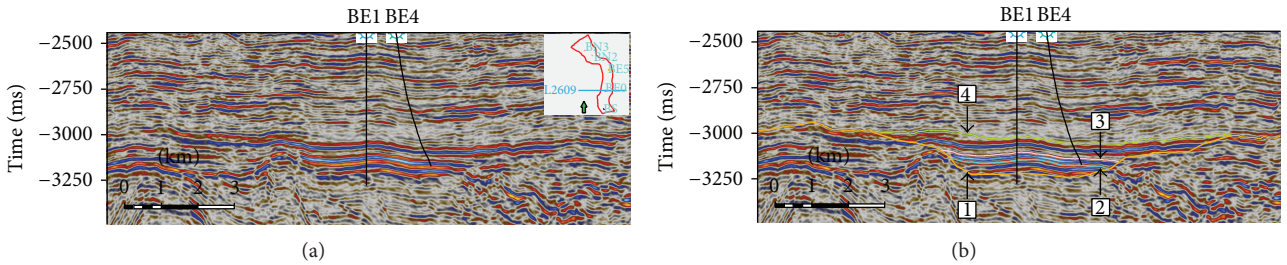

(a) (b)

Figure 8: Uninterpreted (a) and interpreted (b) seismic line number (L 2609) passing through Baltim East field from west to east direction, where (1) bottom Abu Madi, (2) top level III lower, (3) top level II main, and (4) top Abu Madi are picked.

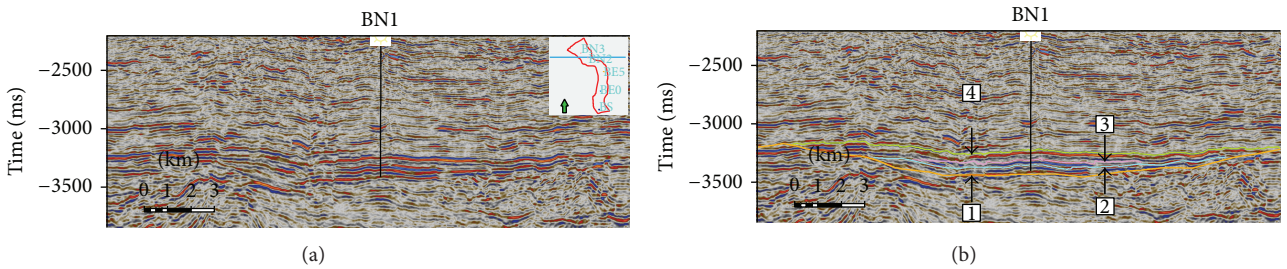

(a) (b)

Figure 9: Uninterpreted (a) and interpreted (b) seismic line number (L 1889) passing through Baltim North field from west to east direction, where (1) bottom Abu Madi, (2) top level III lower, (3) top level II main, and (4) top Abu Madi are picked.

velocity. The reflection's strength changes significantly and is stronger where gas bearing sands determine a strong impedance reduction.

(iii) Top Abu Madi: the interpreted horizon follows a zero crossing value between a strong and continuous through-peak couplet representing a decrease in seismic velocity.

Because of the role faults often play in the entrapment of hydrocarbons, the techniques for finding and mapping faults have considerable importance [15]. Faults planes and their intersections with horizons are digitized from the screen display in a similar way to horizons picking. When a fault is picked on a seismic section, its intersection will appear on an intersecting seismic section. It is much easier to work with faults on lines crossing them approximately at right angle than on lines crossing them obliquely, where the fault plane crosses the bedding at shallow angle. Fault planes and their intersections with horizons are digitized from the screen display in a similar way to horizons picking (Figure 6).

3.3. Velocity and Depth Conversion. Depth conversion of a time interpretation is computationally simple and can be quickly repeated whenever new information becomes available. The physical quantity that relates time to depth is velocity. The velocity required for converting time to depth is the P-wave velocity in the vertical direction. It can be measured directly in a well, or extracted indirectly from surface seismic measurements, or deduced from a combination of seismic and well measurements [17]. In the present study, the check shot survey records and sonic logs were used as a source of the velocity.

The complete interpretation is automatically converted using Petrel software. The workflow of converting data between domains within Petrel is split into two processes:

(i) make velocity model which defines how the velocity varies in space;

(ii) depth conversion which uses the velocity model to move data between domains.

4. Results and Discussion

4.1. Time and Depth Contour Maps. The picked time values and the fault segments locations are posted on the base map of the study area in order to construct structure time maps for the studied horizons (top Abu Madi, top level III main, top level III lower, and bottom Abu Madi). Then, the velocity model is used to convert the reflection time to depths, in order to construct the structure depth maps.

Top Abu Madi has two-way time (TWT) varying between 2871 and 3349 ms, while depth values vary between 3372 and 3651 m (Figure 10). The TWT of level III main reservoir varies between 2972 and 3449 ms, while depth values vary between 3495 and 3815 m (Figure 11) and achieve their maximum value towards the northern corner of the study area. Level III lower reservoir has TWT varying between 3034 and 3532 ms, while depth values vary between 3495 and 3943 m (Figure 12) and achieve their maximum value towards the northern corner of the study area. For bottom Abu Madi the TWT varies between 3034 and 3698 ms, while depth values vary between 3495 and 4185 m (Figure 13). The low-relief areas are located in the northern parts of the study area while the high-relief areas are located towards the south.

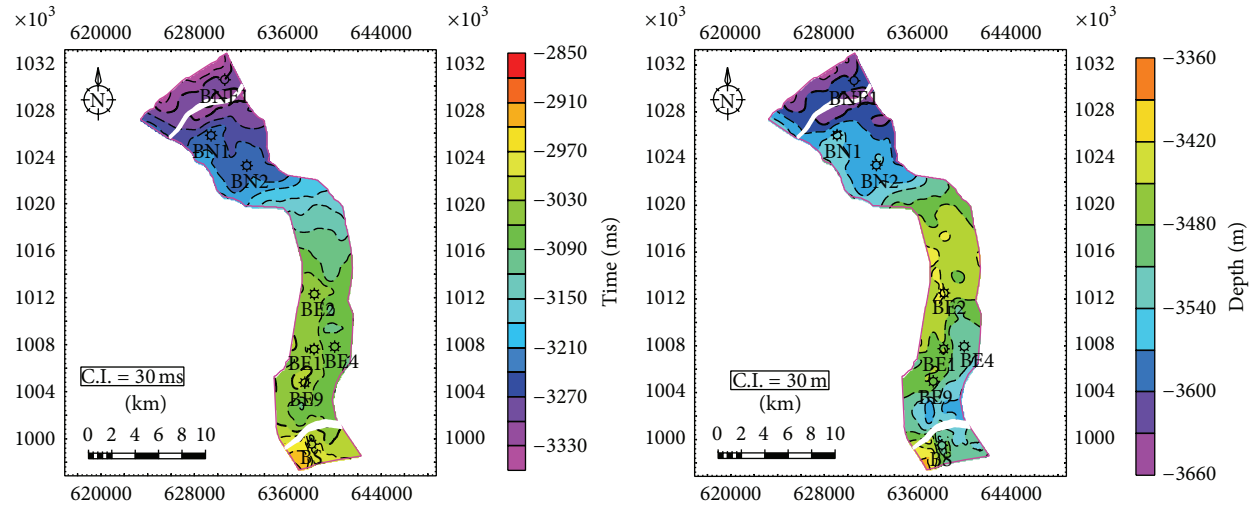

Figure 10: Time and depth structure maps of top Abu Madi Formation.

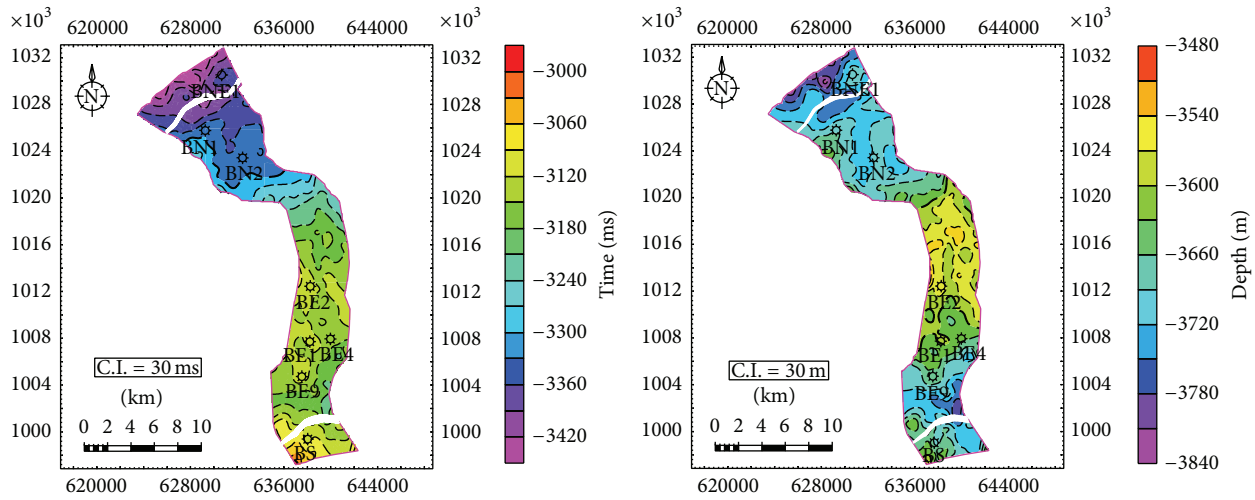

Figure 11: Time and depth structure maps of top level III main horizon.

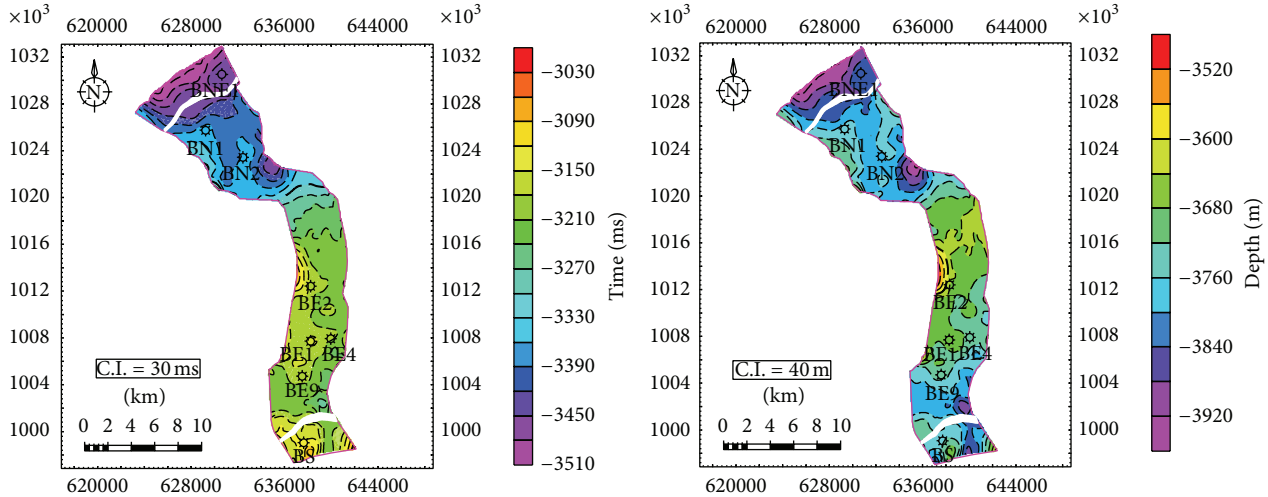

Figure 12: Time and depth structure map of top level III lower horizon.

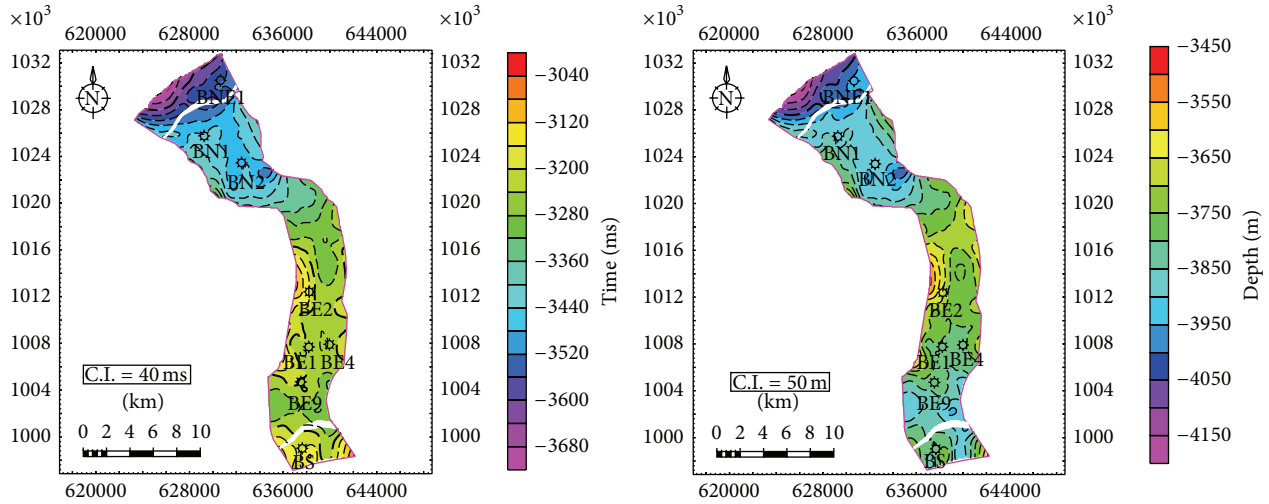

Figure 13: Time and depth structure map of bottom Abu Madi Formation.

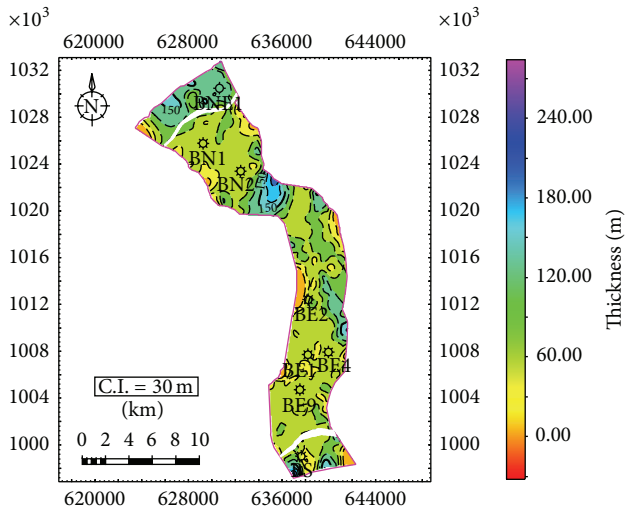

Figure 14: Thickness map of level III main.

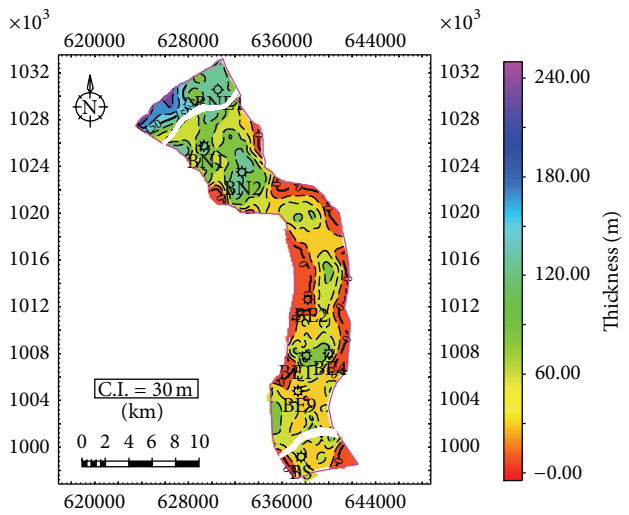

Figure 15: Thickness map of level III lower.

The area was dissected by two main faults (Figure 6): the first one is a great high angle E-W normal fault dipping northward in the southern part of Baltim area between Baltim South and Baltim East fields. The second fault between Baltim North and Baltim Northeast fields, which are in NE-SW direction, dips to the north and displaces all the levels more than 80 m. The time and depth maps of all horizons show that there is a dipping toward the north of the study area as the time and depth values increase toward the north (Figures 10 to 13).

4.2. Isochore Maps. Two isochore thickness maps were constructed for the two pay zones "level III lower" and "level III main." Uncertainties affect these elements throughout the entire interpretation process. They have some bearing on the geometric shape and subsequently on the gross reservoir volume (GRV) of the Baltim fields. The increase of the gross reservoir volume (GRV) leads subsequently to the increase of the net pay thickness, volumes of hydrocarbons in place, reserves, and production profiles. For level III main the thickness varies between 0 and 190 m (Figure 14) while for level III lower the thickness varies between 0 and 210 m (Figure 15). These two isochore maps show that reservoir thickness of both level III main and lower increase at the center of the Abu Madi Paleovalley and pinch-out and decrease toward the boundaries, where the minimum thickness values were observed. Thus, the assessment of geometrical uncertainties is an essential first step in a field study for evaluation, development, or optimization purposes.

4.3. Geological Model. A simplified fluvial sequence stratigraphic model of the Late Messinian Abu Madi Formation is shown in Figure 16. This architecture forms the basic conceptual model of the Abu Madi reservoirs "level III main" and "level III lower," used for well correlation and seismic

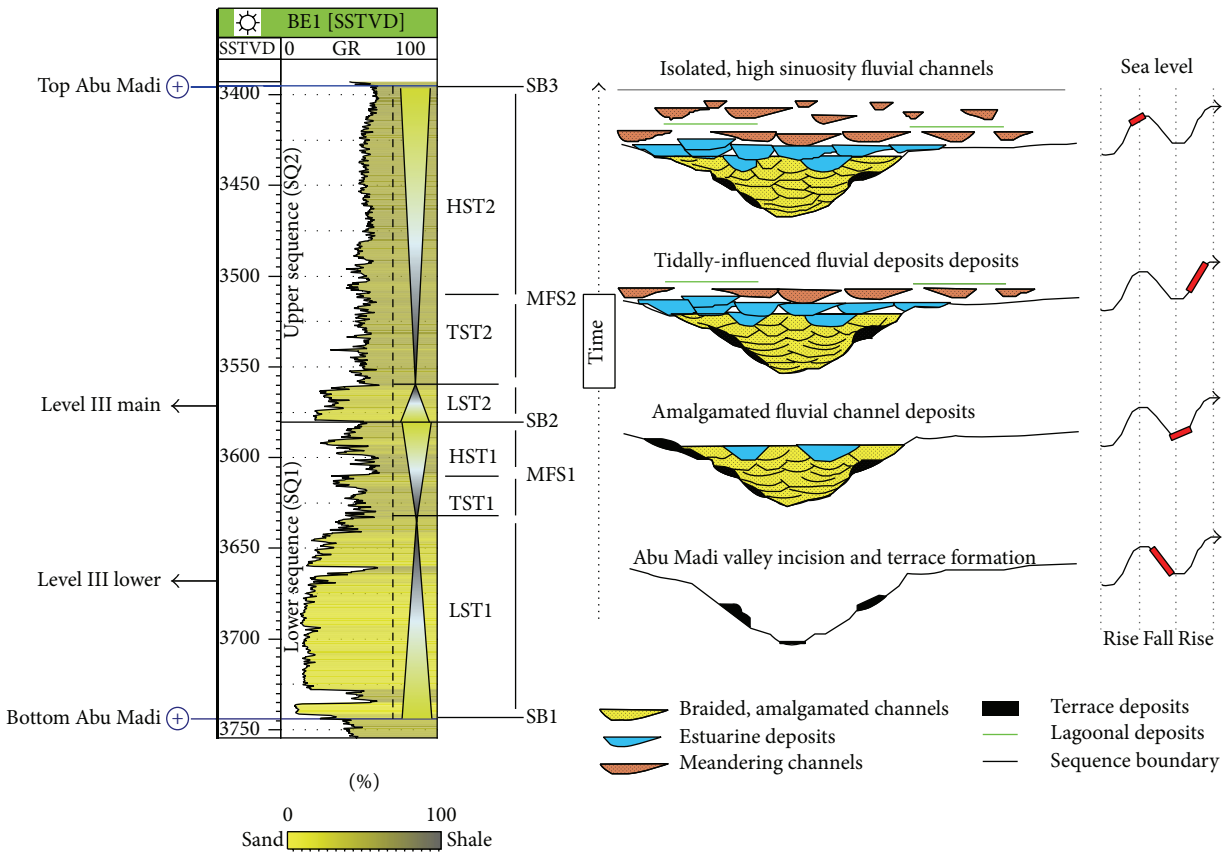

Figure 16: Stratigraphic architecture of a fluvial depositional sequence influenced by base-level fluctuations for the Abu Madi incised valley channel system. Each system tract contains a fining upward succession caused by the continuous coastal aggradation and subsequent shallowing of the fluvial graded profile. List of abbreviations: lowstand system tract (LST), transgressive system tract (TST), highstand system tract (HST), maximum flooding surface (MFS), and sequence boundary (SB).

interpretation. The spatial and temporal relation between braided and meandering river systems is illustrated for a single base-level cycle. At the beginning of the lowstand system tract (LST), braided systems develop close to the source area where the slope is generally steeper, sediment coarser, channels are overloaded, and accommodation is low. Towards the coastal plain as the fluvial slope becomes flatter, meandering systems take over. Rivers here carry less sediment, are underloaded, and therefore usually have single channels. As their sinuosity increases the stresses on the banks raise the probability of bank undermining, out-of-channel flow, and overbank escape of sediments. This meandering system eventually grades into the estuary or delta front systems. Also, due to the overall rise and flattening of the fluvial gradients the entire cycle has a fining upward tendency. But due to the interaction between sediment supply and the rate of accommodation creation at the shoreline the entire system progrades or retrogrades during the three stages of base-level rise. Furthermore, two sudden facies shifts may be present during the base-level rise cycle.

As apparent from Figure 16 transgressions in fluvial systems may cause estuarine or lagoonal deposits, but more often they are associated with a higher occurrence of floodplain deposits when a marine influence remains restricted to areas further basinwards. Floodplain deposits are hardly ever continuous over large areas, due to avulsions and channel migrations [18–20]. Also, overbank deposits and crevasse splays may hinder successful floodplain identification. It is therefore often difficult and unreliable to correlate fluvial sequences based on maximum flooding surface (MFS). This opposed to the marine realm where the MFS is often better developed than the sequence boundary (SB) simply due to the fact that subaerial erosion does not extend below the sea level. In fluvial settings the development of erosional surfaces can be highly heterogeneous due to incisions, but their preservation potential is much higher due to the increasing accommodation following the base-level lowstand. This in contrast to the MFS, which is trailed by a usually thin sand layer developed the highstand system tract (HST) and subsequent base-level fall. It is therefore a common practice to correlate fluvial succession based on SBs and devise a sequence stratigraphic framework in accordance with this.

4.4. 3D Geometric Modeling. Reservoir modeling is playing an increasingly important role in developing and producing hydrocarbon reserves. Various technologies used to understand a prospective reservoir provide information at many different scales. Core plugs are a few inches in size. Well

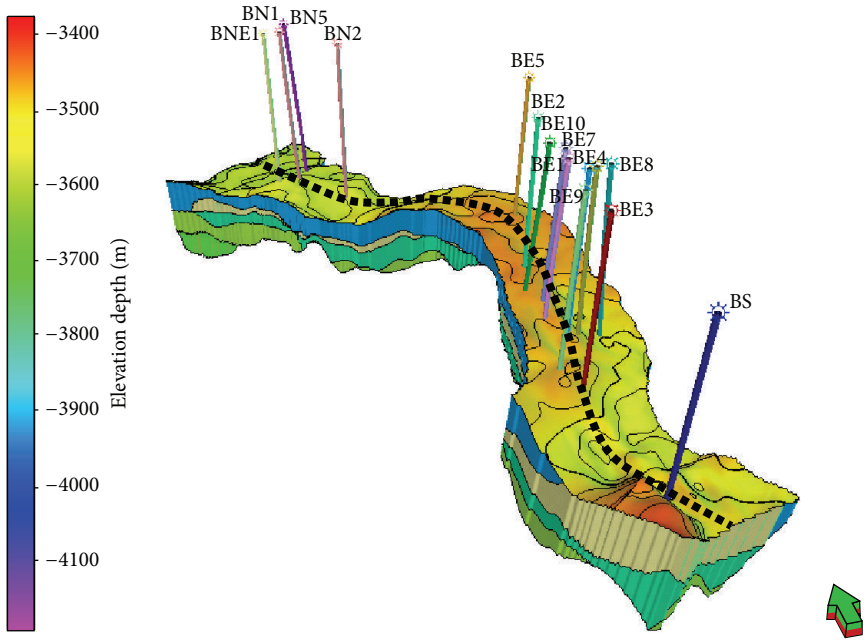

Figure 17: 3D geometric model of Abu Madi reservoirs showing the promising pathway (red dashed line) of the future development wells, which coincides with the up-to-date locations of drilling wells in the Baltim area.

logs can detect properties within a few feet around the well. Seismic imaging covers a huge volume, but its typical resolution is limited to a few meters vertically and tens of meters horizontally [21]. Limited by time and capital, direct sampling of reservoir rock and fluid properties is sparse. Therefore, geologic interpretations based on seismic information and understandings of sedimentary processes are used to interpolate or extrapolate the measured data in order to yield complete reservoir geometry descriptions. Information provided by these technologies is incorporated into reservoir models. Constructing reservoir models has become a crucial step in resource development as reservoir modeling provides a venue to integrate and reconcile all available data and geologic concepts [21].

One of the key challenges in reservoir modeling is accurate representation of reservoir geometry, including the structural framework (i.e., horizons/major depositional surfaces that are nearly horizontal, and fault surfaces which can have arbitrary spatial size and orientation), and detailed stratigraphic layers (Figure 17). The structural frameworks delineate major compartments of a reservoir and often provide the first order controls on in-place fluid volumes and fluid movement during production. Thus, it is important to model the structural frameworks accurately. However, despite decades of advances in grid generation across many disciplines, grid generation for practical reservoir modeling and simulation remains a daunting task.

In typical structural modeling workflows, the first task is to build a fault network as a set of surfaces and contacts between these surfaces. This step is itself decomposed into surface fitting, which creates one fault surface from each fault interpretation, and editing in which faults can be extended, filtered, and connected one to another based on proximity and modeler's interpretation. Then, horizons are built from seismic picks conformably to the fault network [22]. Fault modeling within Abu Madi reservoirs is a reasonably straightforward process since only two faults were identified during the seismic interpretation. Potential synsedimentary faults and slumps are apparent within the reservoir but these were not modeled as they are small in scale and exhibit limited throws. The faults are all normal displacement and were modeled using a network in which individual fault geometries were classified and their interaction defined. Grid-building takes the fault model described above and constructs a 3D grid within the framework of the reservoir-defining seismic surfaces. Seismic surfaces, representing top Abu Madi, top level III main, top level III lower, and bottom Abu Madi, were depth-converted as a part of the interpretation process within Petrel software.

The final result is a 3D geometric model of Abu Madi reservoirs based on well and seismic data (Figure 17) and involves the construction of the modeling grid using a framework of seismic surfaces, faults, and stratigraphic well ties. 3D geometric model of Abu Madi reservoirs shows the promising pathway of the future development wells based on the integration of seismic and well data in this study, which coincides with the up-to-date locations of drilling wells in the Baltim area and locates at the center of the Abu Madi Paleovalley (Figure 17).

5. Conclusions

In conclusion, we have seen that the role of geometric modeling is becoming more important for exploring reservoir structures. 3D geometric modeling provided a useful means towards understanding the structure of Abu Madi

reservoirs. Baltim fields (South, East, and North) comprise two separate gas pools named "level III lower" and "level III main" within the upper Messinian Abu Madi Formation. The trap is a structural-stratigraphic type with pinch-out against incised Abu Madi Paleovalley boundaries and is fault-bounded in the northern and southern part. Identification of stratigraphic architecture not only helps understand the geological history, but also has implications for hydrocarbon exploration as the confinement of flow in an incised valley has great implications for channel amalgamation and produces favorable reservoirs with potential two-way closure. The Abu Madi reservoirs shape influences the seismic response of the incised Abu Madi Paleovalley, making it necessary to account for 3D effects in order to obtain accurate results. The accuracy of the estimated thickness of each Abu Madi reservoir is a critical element in assessment of reserves, volumes of hydrocarbons in place, and production profiles. The promising locations of the future development wells based on the integration of seismic and well data coincide with the up-to-date locations of drilling wells in the Baltim area and locate at the center of the Abu Madi Paleovalley. 3D geometric model of Abu Madi reservoir in Baltim area should be kept in mind during future field development decisions.

Conflict of Interests

The authors declare that there is no conflict of interests regarding the publication of this paper.

Acknowledgments

The authors wish to express their gratitude to Egyptian General Petroleum Corporation (EGPC) and Belayim Petroleum Company (PETROBEL) for providing the seismic lines, well logs, and other relevant data. Ministry of Higher Education & Scientific Research and Ministry of Petroleum in Egypt are also acknowledged for promoting advancement in research and establishing a possible future linkage between the industry and university. They thank Schlumberger for furnishing the Petrel software for the seismic interpretation.

References

[1] S. Dalla, H. Harsy, and M. Serazzi, "Hydrocarbon exploration in a complex incised valley fill: an example from the late Messinian Abu Madi formation (Nile Delta Basin, Egypt)," *The Leading Edge*, vol. 16, no. 12, pp. 1819–1826, 1997.

[2] Egyptian General Petroleum Cooperation (EGPC), *Nile Delta and North Sinai: A Field, Discoveries and Hydrocarbon Potentials (A Comprehensive Overview)*, Egyptian General Petroleum, Cairo, Egypt, 1994.

[3] M. Alfy, F. Polo, and M. Shash, "The geology of Abu Madi gas field," in *Proceedings of the 11th Petroleum Exploration and Production Conference*, pp. 485–513, Cairo, Egypt, 1992.

[4] I. El Heiny, R. Rizk, and M. Hassan, "Sedimentological model for Abu Madi sand reservoir, Abu Madi field, Nile Delta, Egypt," in *Proceedings of the EGPC 10th Exploration and Production Conference*, pp. 1–38, Cairo, Egypt, 1990.

[5] J. D. Pigott and M. I. Abdel-Fattah, "Seismic stratigraphy of the Messinian Nile Delta coastal plain: recognition of the fluvial Regressive Systems Tract and its potential for hydrocarbon exploration," *Journal of African Earth Sciences*, vol. 95, pp. 9–21, 2014.

[6] R. A. Abu El-Ella, "The Neogene-Quaternary section in the Nile Delta, Egypt: geology and hydrocarbon potential," *Journal of Petroleum Geology*, vol. 13, no. 3, pp. 329–340, 1990.

[7] J. C. Dolson, M. V. Shann, S. Matbouly, C. Harwood, R. Rashed, and H. Hammouda, "The petroleum potential of Egypt," *AAPG Memoir*, vol. 74, pp. 453–482, 2001.

[8] M. I. Abdel-Fattah and R. M. Slatt, "Sequence stratigraphic controls on reservoir characterization and architecture: case study of the Messinian Abu Madi incised-valley fill, Egypt," *Central European Journal of Geosciences*, vol. 5, no. 4, pp. 497–507, 2013.

[9] J. Harms and J. Wray, "Nile Delta," in *Geology of Egypt*, R. Said, Ed., pp. 329–343, A. A. Balkema, Rotterdam, The Netherlands, 1990.

[10] M. H. Mohamed, *Evaluation of hydrocarbon potentiality of Miocene rocks in the Northern portion of Abu Madi Paleovalley, offshore Mediterranean Sea, Egypt [M.S. thesis]*, Faculty of Science, Suez Canal University, 2012.

[11] M. I. Abdel-Fattah, "Petrophysical characteristics of the messinian abu madi formation in the baltim east and north fields, offshore Nile delta, Egypt," *Journal of Petroleum Geology*, vol. 37, no. 2, pp. 183–195, 2014.

[12] A. Rizzini, F. Vezzani, V. Cococcetta, and G. Milad, "Stratigraphy and sedimentation of a Neogene-Quaternary section in the Nile Delta area (A.R.E.)," *Marine Geology*, vol. 27, no. 3-4, pp. 327–348, 1978.

[13] M. Bacon, R. Simm, and T. Redshaw, *3-D Seismic Interpretation*, Cambridge University Press, New York, NY, USA, 2003.

[14] M. E. Badley, *Practical Seismic Interpretation*, International Human Resources Development Corporation, Boston, Mass, USA, 1985.

[15] M. B. Dobrin and C. H. Savit, *Introduction to Geophysical Prospecting*, McGraw-Hill, New York, NY, USA, 4th edition, 1988.

[16] O. L. Anderson and J. D. Pigott, "Seismic technology and law: partners or adversaries?" *Energy and Mineral Law Institute*, vol. 24, 2004.

[17] A. R. Brown, *Interpretation of Three-Dimensional Seismic Data*, American Association of Petroleum Geologists and the Society of Exploration Geophysicists, 6th edition, 2004.

[18] O. Catuneanu, "Sequence stratigraphy of clastic systems: concepts, merits, and pitfalls," *Journal of African Earth Sciences*, vol. 35, no. 1, pp. 1–43, 2002.

[19] O. Catuneanu, V. Abreu, J. P. Bhattacharya et al., "Towards the standardization of sequence stratigraphy," *Earth-Science Reviews*, vol. 92, pp. 1–33, 2009.

[20] A. M. Salem, J. M. Ketzer, S. Morad, R. R. Rizk, and I. S. Al-Aasm, "Diagenesis and reservoir-quality evolution of incised-valley sandstone: evidence from the Abu Madi gas reservoirs (upper Miocene), the Nile Delta Basin, Egypt," *Journal of Sedimentary Research*, vol. 75, no. 4, pp. 572–584, 2005.

[21] L. V. Branets, S. S. Ghai, S. L. Lyons, and X.-H. Wu, "Challenges and technologies in reservoir modeling," *Communications in Computational Physics*, vol. 6, no. 1, pp. 1–23, 2009.

[22] G. Caumon, G. Laurent, N. Cherpeau et al., "Structural framework and reservoir gridding: current bottlenecks and way forward," in *Proceedings of the GUSSOW Geoscience Conference*, p. 8, Banff, Canada, 2011.